# Unlubricated Rolling Wear of HNBR/FKM/MWCNT Compounds Against Steel

**D. Xu,[1] J. Karger-Kocsis,[2] Z. Major,[3] R. Thomann[4]**

[1]*Institut für Verbundwerkstoffe GmbH (Institute for Composite Materials), University of Kaiserslautern, D-67663 Kaiserslautern, Germany*
[2]*Faculty of Mechanical Engineering, Department of Polymer Engineering, Budapest University of Technology and Economics, H-1111 Budapest, Hungary*
[3]*Institut für Werkstoffkunde und –prüfung der Kunststoffe, Montanuniversität Leoben, Franz-Josef-Str. 18, A-8700 Leoben, Austria*
[4]*Institut für Makromolekulare Chemie und Freiburger Materialforschungszentrum, Albert-Ludwigs-Universität Freiburg, Stefan-Meier-Str. 31, D-79104 Freiburg, Germany*

Received 20 May 2008; accepted 24 October 2008
DOI 10.1002/app.29513
Published online 5 February 2009 in Wiley InterScience (www.interscience.wiley.com).

**ABSTRACT:** The rolling friction and wear of the compounds of peroxide-cured hydrogenated acrylonitrile/butadiene rubber (HNBR) and fluororubber (FKM) (HNBR-FKM) with and without multiwalled carbon nanotube (MWCNT) contents were studied against steel in orbital rolling ball (steel)-on-plate (rubber) test rig (Orbital-RBOP). The phase structure of the rubber compounds in the presence and absence of MWCNT was studied by dynamic mechanical thermal analysis (DMTA), transmission electron and atomic force microscopy (TEM and AFM, respectively). It was established that HNBR formed the matrix in which micron-scaled FKM domains were dispersed. MWCNT was preferentially embedded in the HNBR. The network-related and surface tension properties of the rubber compounds were derived from DMTA tests and contact angle measurements, respectively. The Martens hardness of the rubbers was also measured. The coefficient of friction (COF) and specific wear rate ($W_s$) were determined in Orbital-RBOP. Blending of HNBR with FKM increased the COF slightly and decreased the specific wear rate prominently when compared with pure HNBR. Additional MWCNT reinforcement (10 parts per hundred part rubber, phr) of the HNBR and HNBR-FKM further increased the COF and at the same time improved the wear resistance. The wear mechanisms were concluded by inspecting the worn surfaces in scanning electron microscope (SEM) and discussed as a function of FKM and MWCNT modifications. © 2009 Wiley Periodicals, Inc. J Appl Polym Sci 112: 1461–1470, 2009

**Key words:** fluoropolymers; nanocomposites; phase behavior; rubber; structure–property relations; rolling wear; carbon nanotube

## INTRODUCTION

Peroxide-cured hydrogenated acrylonitrile/butadiene rubber (HNBR) is preferentially used in many applications because of its outstanding oil and low-temperature resistance. Fluororubber (FKM) is the right selection when superior heat and chemical resistances are needed.[1] Blending of HNBR and FKM can be practiced as their peroxide curing recipe is very similar. Hirano et al.[2] tried this combination to achieve better low-temperature characteristics than the parent materials.

*Correspondence to:* J. Karger-Kocsis (karger@pt.bme.hu).
Contract grant sponsor: DFG (German Research Foundation); contract grant number: GK 814.
Contract grant sponsor: EU Project Kristal; contract grant number: NMP3-CT-2005-515837.
Contract grant sponsor: ElaScreen (Austria).




Carbon nanotube (CNT), discovered by Iijima in 1991,[3] is considered as a promising reinforcement for different polymers. This is due to the high stiffness, strength, and high aspect ratio of the CNTs even in case of their multiwalled variants (MWCNT). The CNT-containing polymer composites have outstanding mechanical performance, strongly improved electric and thermal conductivities if the nanotubes are well dispersed (exfoliated) and well adhered to the matrix.[4] Research works already addressed the potential use of MWCNT for wear-resistant polymeric systems.[5–12]

To combine HNBR with FKM may be an interesting strategy to influence the adhesion component related to friction and wear. Similar to polytetrafluoroethylene, FKM is expected to reduce the coefficient of friction (COF) and enhance the resistance to wear because of its high fluorine content when blended with cocurable rubbers. The prerequisite of cocuring in HNBR/FKM blends is given as their peroxide curing recipes are practically identical.

In our previous work,[13] MWCNT was incorporated into HNBR and this modification was proven to enhance the resistance of the rubber to both sliding and rolling wear. In this work, MWCNT was introduced in compounds containing HNBR and FKM in different ratios, viz. HNBR/FKM = 100/0, 75/25, and 50/50. Effects of the composition ratio and additional MWCNT reinforcement (fixed at 10 part per hundred parts rubber, phr) of the compounds on their rolling friction and wear performance were studied and collated with those achieved on the HNBR systems. The phase structure of the rubber compounds was studied by dynamic mechanical thermal analysis (DMTA), transmission electron microscopy (TEM), and atomic force microscopy (AFM). Wear experiments were carried out in orbital rolling ball-on-plate rig (Orbital-RBOP). The COF and specific wear rate ($W_s$) were determined. The wear mechanisms were concluded by inspecting the worn surfaces in scanning electron microscope (SEM) and discussed in the aspect of FKM and MWCNT modification, respectively.

## EXPERIMENTAL

### Rubber compounds and specimen preparation

The composition of the peroxide-curable HNBR is as follows: HNBR (Therban® LT VP/KA 8882 of Lanxess, Leverkusen, Germany; acrylonitrile content: 21%, Mooney viscosity ML(1+4)100°C = 74) - 100 part; diphenylamine-based thermostabilizer (Luvomaxx CDPA of Lehmann & Voss, Hamburg, Germany) - 1.1 part; zinc-containing mercapto-benzimidazole compound (Vulcanox® ZMB 2/C5 of Lanxess) - 0.4 part; di(*tert*-butylperoxyisopropyl)benzene (Perkadox 14-40 B-PD of Akzo-Nobel, Düren, Germany; active peroxide content: 40%) - 7.5 part; MgO - 2 part; triallyl isocyanurate - 1.5 part; ZnO - 2 part. This mix was produced separately and provided by Lanxess. The curing time of the base mix to reach 90% crosslinking was ca. 10 min at $T = 175$°C.

Peroxide-curable FKM Viton GF-600S of DuPont Performance Elastomers (Geneva, Switzerland) was selected. Its fluorine content is 70 wt % and its Mooney viscosity ML(1+4)121°C = 65. This FKM was added to the ready-to-cure HNBR by setting the following HNBR/FKM ratios: 100/0, 75/25, and 50/50. The related HNBR/FKM mixtures were produced on a two-roll mixing mill (LRM-150BE of Labtech, Bangkok, Thailand) at ca. 50°C by setting a friction ratio of 1.35. To these mixtures, 10 phr MWCNT (Baytubes® C 150 P from Bayer MaterialScience, Leverkusen, Germany) was incorporated in the aforementioned laboratory mill. Note that the cure recipe was not adjusted, i.e., the ready-to-cure HNBR was just diluted by FKM. This means that a direct comparison can only be made between rubber compounds with and without MWCNT filler when their HNBR/FKM ratio is the same.

The rubbers involved in this work are further referred to as HNBR-PURE, HNBR-10MWCNT, HNBR-FKM 75-25, HNBR-FKM 75-25 MWCNT, HNBR-FKM 50-50, and HNBR-FKM 50-50 MWCNT, respectively, in the text.

Curing of the rubbers into 2-mm-thick sheets (100 × 100 mm$^2$ surface) occurred at $T = 175$°C for 15 min in a laboratory press. The specimens for the investigations were cut from these sheets.

### Phase structure of the compounds

#### Dynamic-mechanical thermal analysis

DMTA spectra were measured on rectangular specimens in tensile mode with a constant strain 0.01% with frequency of 10 Hz as a function of temperature (from −100°C to +100°C) using a Q800 device of TA Instruments (New Castle, DE). From −100°C, the temperature was increased stepwise (5°C/step), and for each step the temperature was stabilized for 3 min.

#### Transmission electron microscopy

The phase structure of the rubbers was studied by TEM. TEM measurements were carried out with a Zeiss LEO 912 Omega transmission electron microscopic (Oberkochen, Germany) applying an acceleration voltage of 120 kV. Thin sections (ca. 50 nm) were cut at −120°C with a Diatome diamond knife (Hatfield, PA) using a cryochamber-equipped Ultracut microtome (Reichert and Jung, Vienna, Austria).

#### Atomic force microscopy

AFM analysis was performed in a scanning probe microscope system (Veeco, Santa Barbara, CA) using tapping mode. The Si-tipped cantilever (length = 250 μm, spring constant: ~ 20 N/m) operated at a resonant frequency of ~ 350 MHz during the AFM scans. Amplitude and phase images were taken from the cryofractured surfaces of the rubber compounds. Samples were produced by cutting after immersion in liquid nitrogen.

#### Surface tension and Martens hardness

To check the change in the wettability (surface tension) of the HNBR due to FKM and MWCNT modifications, the sessile drop technique has been adapted. To the surface (cleaned by isopropylalcohol) of the rubber sheets, a drop of double distilled water was placed, and the contact angle was determined using a goniometer of Ramé-Hart (Mountain Lakes, NJ). It was proved that this kind of cleaning

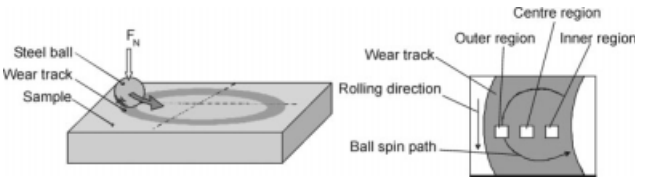


**Figure 1** Scheme of the test configuration of Orbital-RBOP. This figure also shows the preparation of the samples for SEM investigations after Orbital-RBOP test.

did not influence the contact angle data. The reported mean values were derived from at least 10 contact angle measurements.

The Martens (earlier termed to universal) hardness (HU) was determined by the ISO 14577-1 (2002) standard using a Shimadzu DUH 202 device with a Vickers-type diamond indenter.

### Rolling friction and wear

#### Testing

In Orbital-RBOP, the rubber sheet is worn by a steel ball (100Cr6, diameter: 14 mm, arithmetical roughness Ra: 1 μm), which rolls along a circular path (diameter: 33 mm) when pushed against the rubber sheet with a given load. The parameters: load: 90 N, revolution: 280 rpm, duration: 3 h were set for this configuration. This device could record the COF as a function of time. The specific wear rate was calculated by

$$W_s = \frac{\Delta V}{F \cdot L} \quad (1)$$

where $\Delta V$ ($mm^3$) is the volume loss, $F$ (N) is the normal load, $L$ (m) is the overall rolling distance. The loss volume ($\Delta V$) was computed by measuring of the width and depth of the wear track, assessed by a white light profilometer (specified later) with the approximation that the cross section of the wear track was a half ellipse.

The test setup of this testing method is depicted schematically in Figure 1.

#### Wear mechanisms

The worn surfaces were inspected in a MicroProf white light profilometer (Fries Research and Technology, Bergisch Gladbach, Germany) and in SEM (JSM-6300 of Jeol, Japan). The specimens were sputtered with an Au/Pd alloy in a device of Balzers (Lichtenstein) prior to SEM investigation at high acceleration voltages.

## RESULTS AND DISCUSSION

### Phase structure

#### DMTA response

Figure 2 demonstrates the change of the storage modulus ($E'$) and loss factor (tan δ) as a function of the temperature ($T = -100$ to 100°C) for selected compounds, i.e., HNBR-PURE, HNBR-10MWCNT, -FKM 50-50, and -FKM 50-50 MWCNT. One can clearly see that the incorporation of FKM reduces, whereas MWCNT increases the stiffness of the related compounds. Even in case of the logarithmic plot of $E'$ as a function of $T$, one can see that the stiffness increases with decreasing temperature for all systems. This kind of behavior can be traced to the presence of a less tightly crosslinked rubber. The stiffness reduction owing to the introduction of FKM into HNBR may be linked with the curing. Note that

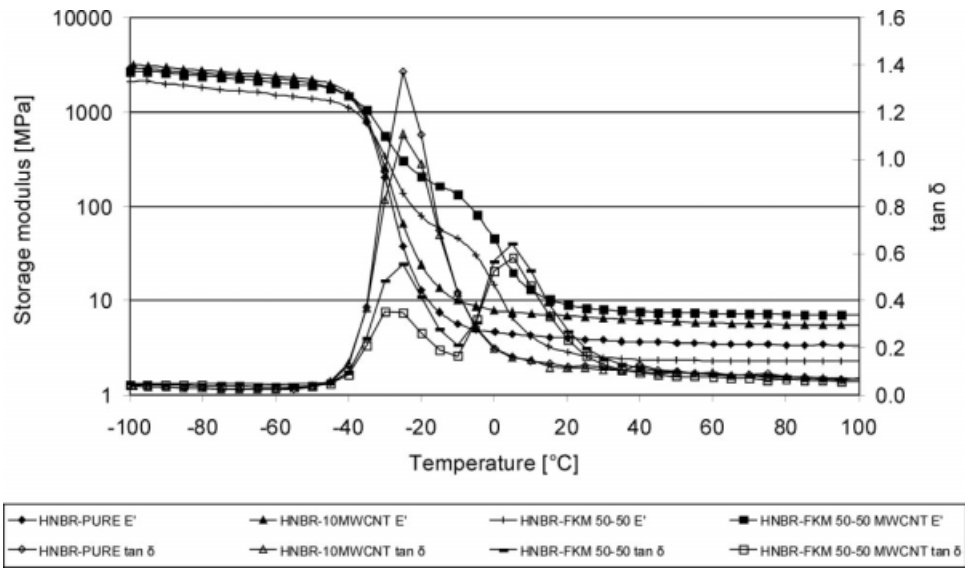


**Figure 2** Storage modulus and loss factor as a function of the temperature for HNBR-FKM with and without MWCNT.

**TABLE I**
**Characteristics of the HNBR and HNBR-FKM Rubber Mixes**

| | HNBR-PURE | HNBR-10MWCNT | HNBR-FKM 75-25 | HNBR-FKM 75-25 MWCNT | HNBR-FKM 50-50 | HNBR-FKM 50-50 MWCNT |
|---|---|---|---|---|---|---|
| $E_{pl}$ at 25°C (MPa) | 3.91 | 6.69 | 2.76 | 9.02 | 2.62 | 8.32 |
| $M_c$ (g/mol) | 2,010 | 1,175 | 3,088 | 1,068 | 3,715 | 1,182 |
| $\nu_c$ (mol/m$^3$) | 526 | 900 | 371 | 1,213 | 352 | 1,119 |
| tan δ at $T_g$ (at −25°C/+5°C) | 1.37 | 1.11 | 1.16/0.31 | 0.36/0.56 | 0.56/0.64 | 0.35/0.58 |
| Density (g/cm$^3$) | 1.057 | 1.057 | 1.146 | 1.296 | 1.309 | 1.322 |
| HU (MPa) | 1.45 | 2.16 | 1.12 | 2.21 | 1.11 | 2.97 |
| Contact angle [°] | ≈102 | ≈99 | ≈95 | ≈90 | ≈98 | ≈90 |

the peroxide curing recipe was not adjusted for the HNBR-FKM mixes—so the content of the curatives has been halved for the HNBR-FKM 50-50. Furthermore, we assume that the curing processes of HNBR and FKM are running parallel, which is hardly the case. Moreover, the interfacial adhesion between HNBR and FKM may be poor. However, these aspects were not addressed in this work.

The peaks in the tan δ vs. $T$ traces at −25 and +5°C can be assigned to the glass transition temperatures ($T_g$) of the HNBR and FKM, respectively. Note that their position does not change with either the HNBR/FKM composition or MWCNT content. Accordingly, these HNBR-FKM mixes are two-phase systems. Based on the fact that the stiffness of the HNBR-FKM compounds drops at the $T_g$ of the HNBR, one can surmise that the latter forms the matrix and FKM is present as dispersed phase within. A closer look at the tan δ vs. $T$ traces allow to make a further working hypothesis in respect to the phase structure. In contrast to the HNBR, the $T_g$ relaxation transition of the FKM is not affected by the MWCNT. The strong reduction of the $T_g$ peak of HNBR owing to MWCNT presence suggests that the MWCNT is located in the HNBR phase preferentially.

According to the rubber elasticity theory, the inverse of the plateau modulus ($1/E_{pl}$) at a given temperature above the $T_g$ is related to the apparent mean molecular mass between crosslinks ($M_c$):

$$E_{pl} = \frac{3 \cdot \rho \cdot R \cdot T}{M_c} \quad (2)$$

where $E_{pl}$ is the modulus at an absolute temperature above the $T_g$ (in this case above that of the FKM, i.e., at 298 K), ρ is the density, $R$ is the universal gas constant [8.314 J/(K mol)], and $T$ is the absolute temperature (e.g., $T = 298$ K).

Alternatively, one can consider the apparent network density ($v_c$) given by:

$$v_c = \frac{\rho}{M_c} \quad (3)$$

The network-related data, which are rough estimates as morphological and filler-related parameters were not considered, are summarized in Table I. One can recognize that $M_c$ decreases and $v_c$ increases dramatically when MWCNT is added to the related compound. However, FKM in the compounds has a reverse effect. Again, this may be due to the effects of the curing recipe (being "diluted" when adding FKM to the HNBR) and difference in the cure rates between HNBR and FKM. Nonetheless, because of the presence of FKM in the HNBR, the overall apparent crosslink density of the related compound is lower than that of the plain HNBR.

Data in Table I indicate that the incorporation of MWCNT and FKM enhances the density of HNBR-PURE and HNBR-FKM materials, respectively. The Martens hardness of the pure and blended HNBR systems increases prominently with the addition of MWCNT. The introduction of FKM to HNBR decreases the HU as expected. It is interesting to note that the HU data of the MWCNT-containing HNBR-FKM compounds is somewhat higher than that of the HNBR-10MWCNT. This can be explained by assuming that the MWCNT is predominantly present in the HNBR matrix.

## TEM, AFM, and contact angle results

TEM pictures taken from the HNBR-FKM 50-50 clearly show that the FKM is dispersed in the continuous HNBR phase (cf. Fig. 3). The FKM is present in the form of large micron-scaled domains in the HNBR matrix. This phase structure does not change by the incorporation of MWCNT (cf. Fig. 4). Moreover, one can clearly recognize that MWCNT is preferentially embedded in the HNBR matrix. This finding is in line with the DMTA data and hardness results discussed before. The TEM pictures in Figure 4 also display that the MWCNTs are poorly dispersed, the nanotubes remained highly entangled in the form of large agglomerates in the HNBR phase of the HNBR-FKM 50-50 mix. Nonetheless, MWCNT may still work as a useful tribological additive, as already demonstrated in our former work.[13] Comparing the high-magnification AFM phase images taken from the HNBR-FKM 50-50 and HNBR-FKM 50-50

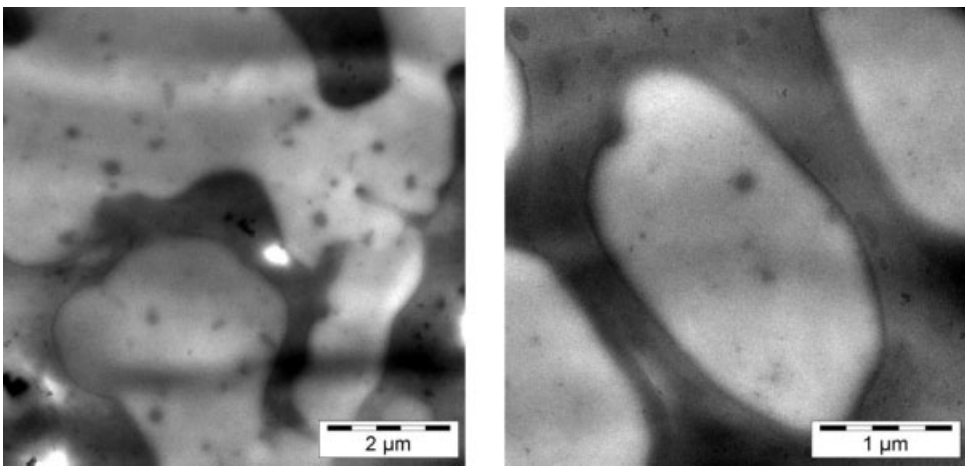


**Figure 3** TEM pictures taken from the HNBR-FKM 50-50 compound.

MWCNT, one can notice that the phase structure of the blend did not change by the introduction of MWCNT (cf. Fig. 5). MWCNT-rich domains are well resolved in the HNBR phase in the AFM phase image of the HNBR-FKM 50-50 MWCNT. Although we did not succeed to resolve MWCNTs separately by AFM, the dark domains in the related phase image in Figure 6 can clearly be assigned to MWCNT-rich agglomerates, which are dispersed in the HNBR phase. This assignment is supported by the TEM results. Recall that the size of the domains in Figure 6 agrees fairly with those that represent MWCNT agglomerates according to TEM images in Figure 4.

Results of the contact angle measurements show that the incorporation of FKM into HNBR yielded some slight reduction in the contact angle (cf. Table I). Additional modification by MWCNT resulted in some further decrease in the contact angles. The contact angle data are similar to those published for HNBR[14] and some fluorinated latex systems.[15] Note that this finding, for which no simple explanation can be given at present, is against the expectation. Ikeda et al.[16] modified HNBR by copolymerization with fluoro-containing acrylates via peroxide crosslinking of the HNBR. The authors found that the surface tension of the HNBR was reduced by this way. This finding agreed with our working hypothesis, viz. HNBR blending with FKM would increase the contact angle that would reduce the adhesion component of friction, and finally reduce the COF. This was, however, not the case. The highly viscous FKM, being dispersed in the HNBR, did not enrich at the surface layer against the expectation.

### Friction and wear

The COF and $W_s$ of HNBR and HNBR-FKM with and without MWCNT measured in Orbital-RBOP are summarized in Figure 7. One can get the impression that the compounds of HNBR and FKM have higher COF and markedly lower $W_s$ when compared

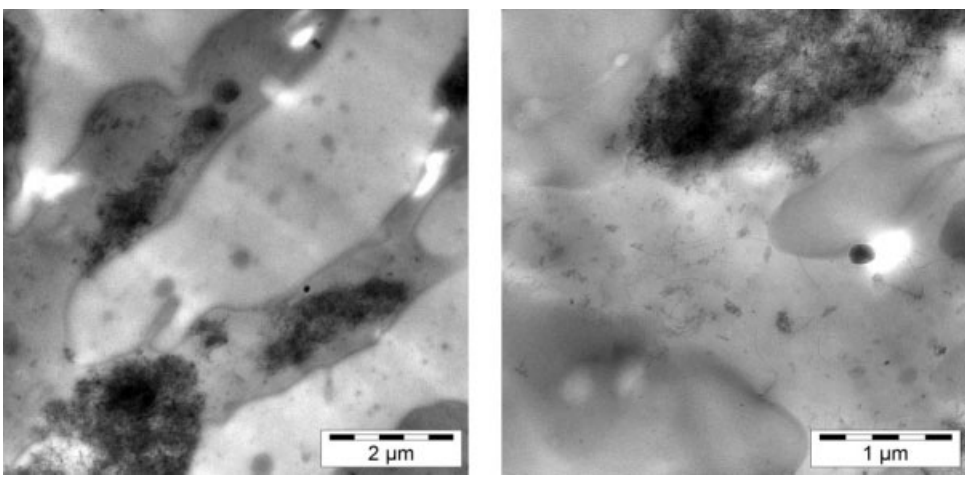


**Figure 4** TEM pictures taken from the HNBR-FKM 50-50 MWCNT compound.

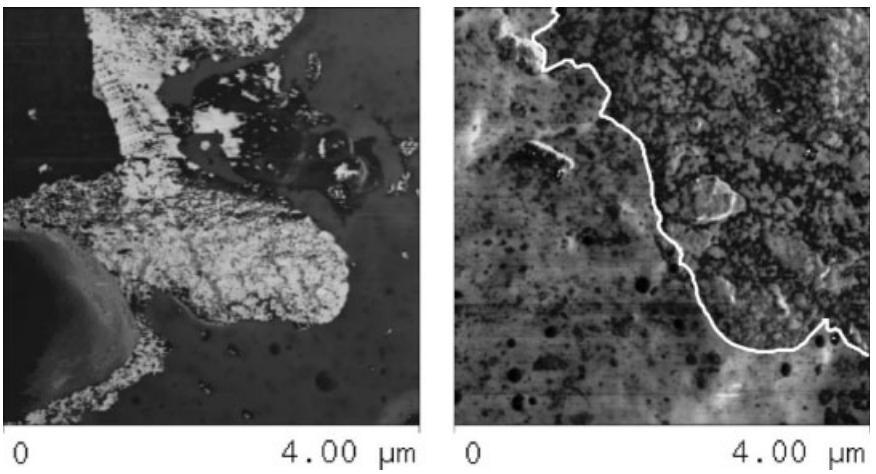


**Figure 5** AFM phase images taken from the cryocut surface of HNBR-FKM 50-50 (left) and HNBR-FKM 50-50 MWCNT (right). Note: the bright phase in the sample HNBR-FKM 50-50 represents FKM. The white continuous line in the image of HNBR-FKM 50-50 MWCNT separates the HNBR (left-hand side) from that of the FKM (right-hand side). The former, i.e. HNBR, contains the agglomerated MWCNT.

with HNBR-PURE. The more FKM the compound contains, the higher is the COF. This tendency in COF can be traced to the change observed for the contact angles (cf. Table I). Increasing wettability, represented by smaller contact angles, should be accompanied with increased adhesion during friction and thus manifest in enhanced COF.

The specific wear rate does not show monotonous decrease with the increasing content of FKM. HNBR-FKM 75-25 has better rolling wear resistance than HNBR-PURE and HNBR-FKM 50-50. However, remember that HNBR and HNBR-FKM compounds are not directly comparable as the curatives became less and less with increasing FKM content. Incorporation of MWCNT into HNBR-FKM increases the COF (which corroborates the proposed correlation between COF and contact angle) and further decreases the specific wear rate.

## Wear mechanisms

Figure 8 shows the SEM pictures taken from the rolling wear tracks of HNBR-PURE and HNBR-10MWCNT. As the ball in the test setup is guided by a bearing ring, fixed at a motor shaft, it spins additionally when rotates with concentric revolutions. As a result, the wear track could be different and divided into three regions (cf. Figure 1).[13] Figure 8(a,b,e,f ) show the worn surfaces of the regions with additional forward (outer region, cf. Fig. 1) and backward spins of the ball (inner region, cf. Fig. 1), respectively. Figure 8(c,d) are from the midpart between the outer and inner regions (center region, cf. Fig. 1). A detailed analysis on the wear mechanisms for similar HNBR systems can be found in the previous article.[13] The SEM pictures displayed here help to compare the wear mechanisms of HNBR with those of HNBR-FKM with and without MWCNT.

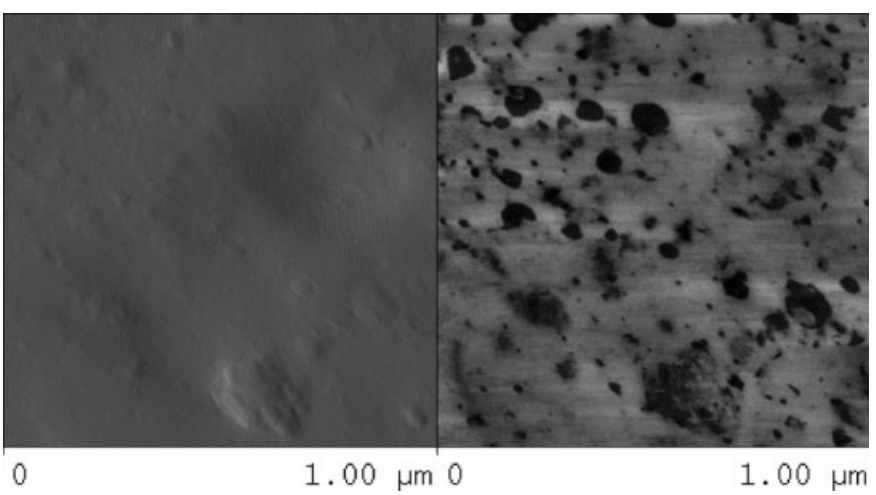


**Figure 6** AFM amplitude (left) and phase images (right) from the cryocut surface of the HNBR-FKM 50-50 MWCNT showing MWCNT agglomerates in the HNBR phase.

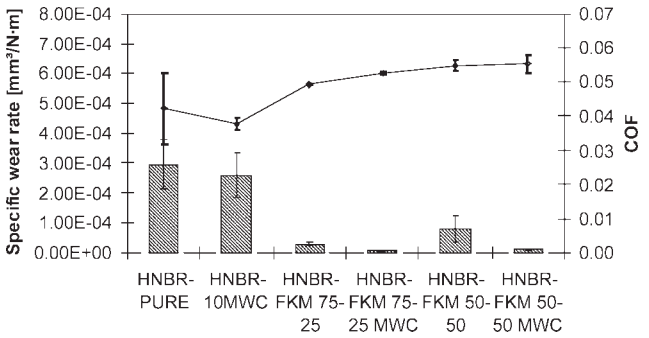


**Figure 7** Changes of COF (line) and specific wear rate (column) of different HNBR-FKM with and without MWCNT in Orbital-RBOP.

SEM pictures taken from the rolling wear tracks of HNBR-FKM 75-25 with and without MWCNT after Orbital-RBOP tests are shown in Figure 9. In the outer region of HNBR-FKM 75-25, Schallamach type pattern[17] appears with some fragments [cf. Fig. 9(a)]. Clusters from debris (agglomerates) were formed in the center and inner regions [cf. Fig. 9(c)]. Incorporation of MWCNT changes the basic wear mechanisms in the outer region [cf. Fig. 9(b)]. Fatigued-induced formation of holes becomes the main wear mechanism instead of the Schallamach wavy pattern in HNBR-FKM 75-25. Hole development and debris clustering were found in the center region of HNBR-FKM 75-25 MWCNT [cf. Fig. 9(b)]. Fatigue-induced

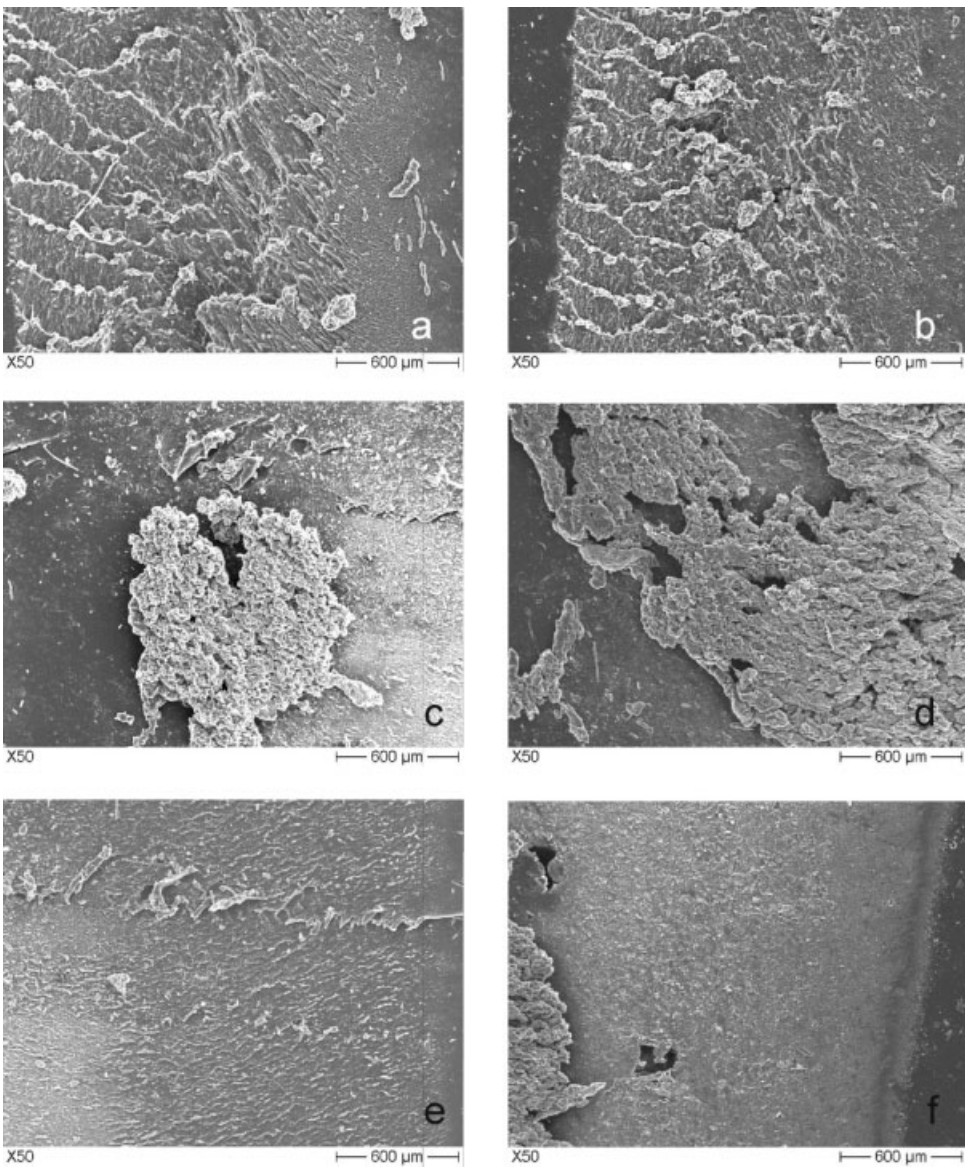


**Figure 8** SEM pictures taken from the rolling wear tracks of HNBR-PURE (a, c, and e) and HNBR-10MWCNT (b, d, and f) after Orbital-RBOP tests; (a and b) outer region, (c and d) center region, (e and f) inner region. Note: rolling direction is downward.

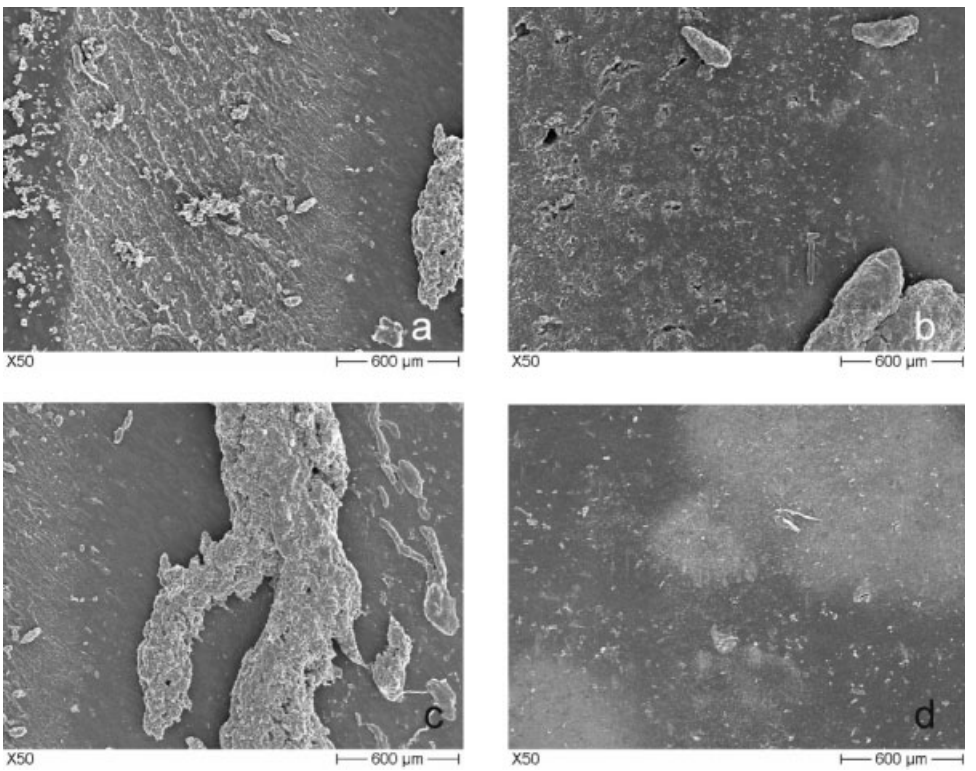


**Figure 9** SEM pictures taken from the rolling wear tracks of HNBR-FKM 75-25 without (a and c) and MWCNT with (b and d) after Orbital-RBOP tests; (a) outer region, (b) outer and center regions, (c) center and inner regions, (d) inner region. Note: rolling direction is downward.

pittings and small "ironed" particles are seen in the inner region of the HNBR-FKM 75-25 MWCNT [cf. Fig. 9(d)].

The wear mechanisms for the HNBR-FKM 50-50 (MWCNT) did not change practically when compared with HNBR-FKM 75-25 (MWCNT) (cf. Fig. 10). However, the inner region of HNBR-FKM 50-50 is full with "ironed" rolls, debris [cf. Fig. 10(c)].

One may notice the changes of the wear mechanisms caused by the introduction of FKM. The incorporation of FKM inhibits the formation of the Schallamach pattern. The space between the neighboring waves and the height of the wave are reduced in the outer region, and the Schallamach pattern disappears in the inner region with increasing FKM content in the HNBR-FKM systems. No rolls are observed at the heads of the waves in HNBR-FKM. Recall that Schallamach waves with prominent roll formation were present in the inner region [cf. Fig. 8(e,f)] of the HNBR systems. However, as underlined earlier, HNBR and HNBR-FKM compounds cannot be compared directly because the curatives became less and less with increasing FKM content. Nevertheless, this finding is quite unexpected as rubbers, when becoming "softer," tend to fail by this kind of wavy pattern during unlubricated sliding and rolling wear tests (e.g., Refs. 18 and 19). One possible reason behind this behavior is a poor interfacial bonding between the HNBR and FKM phases.

By comparing the worn surfaces of HNBR-FKM with and without MWCNT, we notice that the Schallamach wavy pattern disappears after MWCNT introduction. This change in the wear mechanism reflects a reduction in the specific wear rate, which was found in this work. It is worthnoting that the Schallamach-type wear disappears with increasing reinforcement of a rubber independent of the type of the active filler used.[18,19]

Clusters of debris are formed in the center regions for all samples inspected in this work. Note that the effect of the spin of the ball is negligible in the center region. The debris produced in the outer and inner regions were likely swept into the center region by the spin of the ball favoring the formation of such agglomerates.

Note that the dilution of the curing recipe cannot be made responsible alone for the nonmonotonous changes in the friction and wear properties of the compounds with increasing content of FKM. Hirano et al.[2] indicated that several dynamical mechanical properties of HNBR-FKM (storage modulus, peak temperature of the loss modulus) did not follow the additivity rule in respect with the composition.

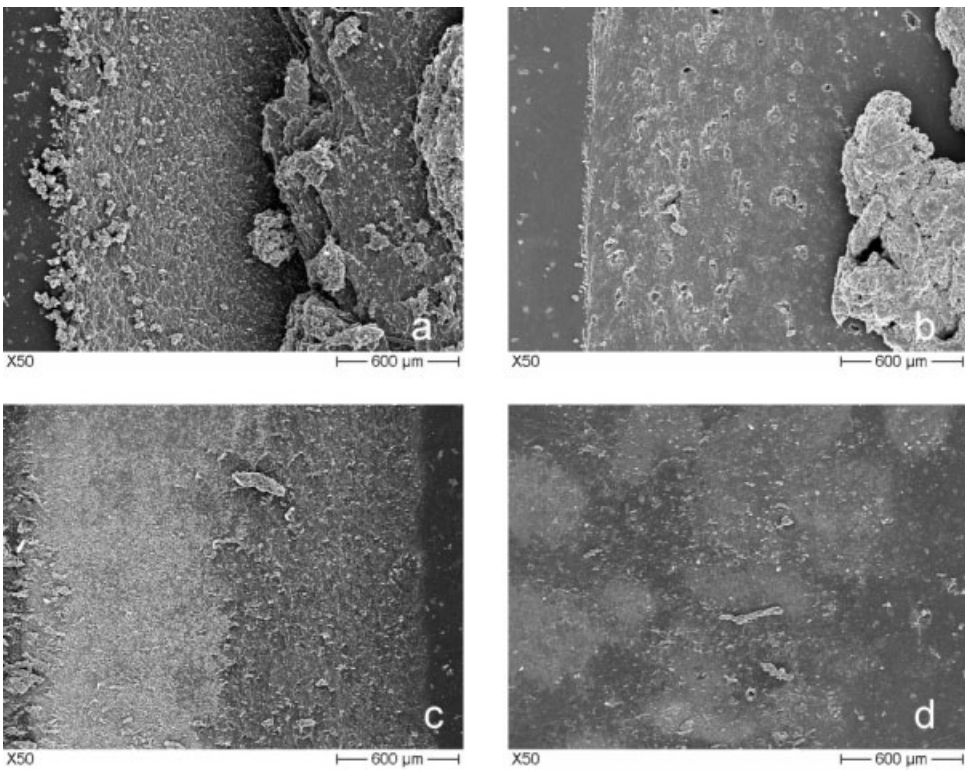


**Figure 10** SEM pictures taken from the rolling wear tracks of HNBR-FKM 50-50 without (a and c) and with (b and d) MWCNT after Orbital-RBOP tests; (a and b) outer and center regions, (c and d) inner region. Note: rolling direction is downward.

## CONCLUSIONS

HNBR and FKM mixes (100/0, 75/25, and 50/50) were tested in Orbital-RBOP to investigate their performance under dry rolling conditions. MWCNT was used as reinforcement and its effect on the COF, the $W_s$, and the corresponding rolling wear mechanisms was analyzed. Based on this work, the following conclusions can be drawn:

- Incorporation of FKM reduced, whereas MWCNT increased the stiffness of both HNBR and HNBR-FKM compounds. The latter were two-phase systems: FKM was dispersed in micron-scaled domains in the HNBR matrix. The position of $T_g$ peaks of the rubbers was not affected by either FKM or MWCNT modifications. DMTA, TEM, AFM, and Martens hardness results indicated/evidenced that MWCNT is preferentially embedded in the HNBR matrix. The apparent $M_c$ decreased and $v_c$ increased dramatically by adding MWCNT, whereas FKM produced a reverse tendency. The latter was traced to a change in the curing recipe (note that the curatives were reduced by increasing amount of the FKM in the HNBR/FKM mixes) and to a difference in the cure rates between HNBR and FKM (not studied in this work). Incorporation of FKM and MWCNT slightly reduced the contact angle of the compounds.
- The compounds of HNBR and FKM exhibited slightly higher COF and considerably lower $W_s$ when compared with the plain HNBR. The more FKM the compound contained, the higher was the COF. HNBR-FKM 75-25 had the best rolling wear resistance when compared with HNBR-PURE and HNBR-FKM 50-50. The reinforcement of MWCNT into HNBR-FKM increased the friction and further enhanced the wear resistance. Whether the change in the COF can be traced to the change observed in the contact angles requires further attention.

The authors thank Mr. D. Felhös for his involvement in the DMTA tests.

## References

1. Wikipedia. Available at http://en.wikipedia.org/wiki/Main_Page (accessed May 2008).
2. Hirano, K.; Suzuki, K.; Nakano, K.; Tosaka, M. J Appl Polym Sci 2005, 95, 149.
3. Iijima, S. Nature 1991, 354, 56.
4. Xiong, J. W.; Zheng, Z.; Qin, X. M.; Li, M.; Li, H. Q.; Wang, X. L. Carbon 2006, 44, 2701.
5. Wei, Z.; Zhao, Y. P.; Ruan, S. L.; Gao, P.; Yu, T. X. Surf Interface Anal 2006, 38, 883.

6. Jacobs, O.; Xu, W.; Schädel, B.; Wu, W. Tribol Lett 2006, 23, 65.
7. Chen, H. Y.; Jacobs, O.; Wu, W.; Rudiger, G.; Schädel, B. Polym Test 2007, 26, 351.
8. Enomoto, K.; Yasuhara, T.; Kitakata, S.; Murakami, H.; Ohtake, N. N Diamond Frontier Carbon Technol 2004, 14, 11.
9. Wang, C.; Dong, B.; Gao, G. Y.; Xu, M. W.; Li, H. L. Mater Sci Eng A 2008, 478, 314.
10. Chen, W. X.; Li, F.; Han, G.; Xia, J. B.; Wang, L. Y.; Tu, J. P.; Xu, Z. D. Tribol Lett 2003, 15, 275.
11. Du, J. H.; Bai, J.; Cheng, H. M. Express Polym Lett 2007, 1, 253.
12. Song, H. J.; Zhang, Z. Z.; Men, X. H. Eur Polym J 2007, 43, 4092.
13. Felhös, D.; Karger-Kocsis, J.; Xu, D. J Appl Polym Sci 2008, 108, 2840.
14. Martínez, L.; Álvarez, L.; Huttel, Y.; Méndez, J.; Román, E.; Vanhulsel, A.; Verheyde, B.; Jacobs, R. Vacuum 2007, 81, 1489.
15. Ha, J.-W.; Park, I. J.; Lee, S.-B. Macromolecules 2005, 38, 736.
16. Ikeda, T.; Yamada, B.; Tsuji, M.; Skurai, S. Polym Int 1999, 48, 446.
17. Schallamach, A. Wear 1971, 17, 301.
18. Karger-Kocsis, J.; Mousa, A.; Major, Z.; Békési, N. Wear 2008, 264, 359.
19. Xu, D.; Karger-Kocsis, J.; Schlarb, A. K. J Mater Sci 2008, 43, 4330.